Bioorganic Chemistry 113 (2021) 105025

Contents lists available at ScienceDirect

Bioorganic Chemistry

journal homepage: www.elsevier.com/locate/bioorg

Neuroprotective and anti-inflammatory phenylethanoid glycosides from the fruits of *Forsythia suspensa*

Si-Yuan Shao, Fan Zhang, Ya-Nan Yang, Zi-Meng Feng, Jian-Shuang Jiang, Pei-Cheng Zhang *

State Key Laboratory of Bioactive Substance and Function of Natural Medicines, Institute of Materia Medica, Chinese Academy of Medical Sciences and Peking Union Medical College, Beijing 100050, China

ARTICLE INFO

Keywords:
Forsythia suspensa
Phenylethanoid glycoside dimers
Neuroprotective activity
Anti-inflammatory activity
TNF-α

ABSTRACT

Neuroinflammation is emerging as a crucial reason of major neurodegenerative diseases in recent years. Increasingly evidences have supported that bioactive natural products from traditional Chinese medicines have efficiency for neuroinflammation. *Forsythia suspensa*, a typical medicinal herb, showed potential neuroprotective and anti-inflammatory properties in previous pharmacological studies. In our research to obtain neuroprotective and anti-inflammatory natural products, three unprecedented C6–C7′/C6–C16′ linked phenylethanoid glycoside dimers (**1**–**3**), three new phenylethanoid glycosides (**4**–**6**), and six known compounds (**7**–**12**) were isolated from the fruits of *Forsythia suspensa*. Their structures were determined by comprehensive spectroscopic data and comparison to the literature data. All isolated compounds were evaluated their neuroprotective and anti-inflammatory activities. Compounds **1** and **10** exhibited significant neuroprotective activities with the cell viability values of 75.24 ± 8.05% and 93.65 ± 10.17%, respectively, for the serum-deprivation and rotenone induced pheochromocytoma (PC12) cell injury. Meanwhile, compound **1** exhibited excellent anti-inflammatory activity against tumor necrosis factor (TNF)-α expression in LPS induced RAW264.7 cells with the IC_{50} value of 1.30 μM. This study revealed that the bioactive phenylethanoid glycosides may attenuate neuroinflammation through their neuroprotective and anti-inflammatory activities.

1. Introduction

Neuroinflammation is a natural inflammatory response of the nervous immune system to stimuli such as tissue damage or metabolic derangements. Multiple investigations have proved that neuroinflammation underlies diverse neurodegenerative diseases, including Alzheimer's disease, frontotemporal dementia, Parkinson's disease, amyotrophic lateral sclerosis and Huntington's disease, of which Alzheimer's disease and Parkinson's disease are the first and second most prevalent age-related neurodegenerative disorders in the world. Increasing evidence today suggests that neuroinflammation is not only a later consequence but also could be an early trigger of the pathology [1–4]. However, the clinical therapies available for the treatment of neuroinflammation associated diseases nowadays have massive trouble with their efficiency and safety [5,6].

For the neuroinflammation associated diseases, such as Parkinson's disease, a potential therapy is found agencies both have neuroprotective effect for neurons in the brain and anti-inflammatory activity inhibiting production of inflammatory cytokines [4]. In recent years, an increasing number of studies have indicated that natural products from traditional Chinese medicines with neuroprotective and anti-inflammatory activities have become an excellent option to attenuate neuroinflammation for their efficiency and low toxicity [7–9]. *Forsythia suspensa*, a typical medicinal herb, is widely cultivated throughout the north area of China [10]. Its fruits, Chinese name "liaoqiao", have been traditionally used as Chinese herbal medicine for the treatments of ulcer, scrofula, acute mastitis, erysipelas, stranguria, hyperpyrexia and polydipsia for a long time [11]. Pharmacological investigations showed that its ethanol extract and forsythosides A and B, two main phenylethanoid glycosides of *F. suspensa*, possessed neuroprotective and anti-inflammatory properties [12–14]. Accordingly, this study was designed to isolate more novel and bioactive phenylethanoid glycosides against neuroinflammation from the fruits of *F. suspensa*. As a result, three unprecedented phenylethanoid glycoside dimers (**1**–**3**), three new phenylethanoid glycosides (**4**–**6**), along with six known compounds (**7**–**12**) were obtained from its 75% ethanol extract. Their neuroprotective activities against rotenone or serum-deprivation induced PC12 cell injury and anti-inflammatory activities on inhibition of TNF-α

* Corresponding author.
E-mail address: pczhang@imm.ac.cn (P.-C. Zhang).

https://doi.org/10.1016/j.bioorg.2021.105025
Received 22 February 2021; Received in revised form 18 May 2021; Accepted 24 May 2021
Available online 26 May 2021

production in RAW264.7 cells were evaluated.

2. Experiments

2.1. General experimental procedures

Ultraviolet (UV) spectra were performed on a JASCO V650 spectrometer. Infrared (IR) spectra were recorded on a Nicolet 5700 spectrometer. High-resolution electrospray ionization mass spectroscopy (HRESIMS) was achieved by an Agilent 6520 series LC-Q-TOF mass spectrometer. ESIMS was measured on an Agilent 1100 series LC/MSD TOF mass spectrometer. Nuclear magnetic resonance (NMR) spectra were recorded by Bruker 500 MHz spectrometer and the values were given in ppm. Optical rotations were measured on a JASCO P-2000 polarimeter. Electronic circular dichroism (ECD) spectra were recorded on a JASCO J-815 chirascan. The semi-preparative high performance liquid chromatography (HPLC) experiments were carried out by Shimadzu LC-10AT equipped with an SPD-10A detector using an YMC-Pack ODS-A column (20 mm × 250 mm, 5 μm). Gas chromatography (GC) analysis was performed using an Agilent 7890A series system with a capillary column, HP-5 (60 m × 0.25 mm, with a 0.25 μm film). Column chromatographic isolations were performed using macroporous adsorption resin (Diaion HP-20, Mitsubishi Chemical Corp., Tokyo, Japan) and Sephadex LH-20 gel (Pharmacia Fine Chemicals, Uppsala, Sweden).

2.2. Chemicals and reagents

Methanol (No. 105101) and acetonitrile (No. 101020) for HPLC were purchased from Beijing Chemical Co., Ltd. (Beijing, China). Deuterated dimethyl sulfoxide (No. 296147) for NMR experiments and MTT were the products of SigmaAldrich Chemical Co., Ltd. (Shanghai, China). Analytical chemicals including ethanol (No. 101058), petroleum ether (No. 105117), ethyl acetate (No. 101029), *n*-butanol (No. 105049), pyridine (No. 107001) and *n*-hexane (No. 105055) were purchased from Beijing Tongguang Fine Chemicals Company (Beijing, China). Reagents including L-cysteine methyl ester hydrochloride (No. 269669), *N*-trimethylsilylimidazole (No. 600909), D-glucose (No. 47249), D-xylose (No. 203391) and L-rhamnose monohydrate (No. 581498) were obtained from J&K Scientific (Beijing, China). Fetal bovine serum (FBS, No. 10099141), horse serum (No. 26050088) and Dulbecco's modified Eagle's medium (DMEM, No. 11965118) were purchased from ThermoFisher Scientific (Waltham, MA). PC12 (No. 3111C0001CCC000024) and RAW264.7 (No. 3111C0001CCC000146) cell lines were obtained from the Institute of Basic Medicine of Chinese Academy of Medical Sciences (Beijing, UT). TNF-α ELISA assay kits (No. ml001543) were purchased from Shanghai Enzyme-linked Biotechnology Co., Ltd. (Shanghai, China).

2.3. Plant material

The fruits of *F. suspensa* were collected from Yuncheng City, Shanxi Province, China, in 2011. The Chinese herbal medicine was identified by Prof. Lin Ma. A voucher specimen (ID-S-2597) has been deposited at the Herbarium of Department of Medicinal Plants, Institute of Materia Medica, Chinese Academy of Medical Sciences, Beijing.

2.4. Extraction and isolation

The dried fruits of *F. suspensa* (90 kg) were extracted for three times with 75% C_2H_5OH under reflux to produce crude extract (12.6 kg). The extract was suspended in water and successively partitioned with petroleum ether (3 × 30 L), ethyl acetate (3 × 30 L) and *n*-butanol (3 × 30 L), respectively. The four portions were evaluated for their neuroprotective activities on rotenone induced PC12 cells and the *n*-butanol portion exhibited the most significant neuroprotective effect with 78.5 ± 5.0%. Then, the *n*-butanol section (4 kg) was suspended in water to obtain an aqueous layer (1.5 kg) and a water insoluble portion (2.5 kg). The assays showed that the aqueous layer possessed better neuroprotective effect of 72.5 ± 1.4% than that of the water insoluble portion. Thus, the aqueous layer was evaporated and chromatographed on a macroporous adsorption resin column, eluting with a mixture of C_2H_5OH–H_2O (0%, 15%, 30%, 50% and 95%) to afford five fractions. The five fractions were tested for their neuroprotective effects. The 30% and 50% ethanol portions showed the effects of 85.2 ± 6.2% and 72.5 ± 7.3%, respectively. Considering the 30% ethanol portion has been studied before, we chose the 50% ethanol portion in this research [15].

The 50% ethanol portion (392 g) was chromatographed on a small macroporous adsorption resin column, eluting with a step mixture of C_2H_5OH–H_2O (0%–95%) to afford seven fractions (Fr. I–VII). Fr. V (180 g) was performed on a Sephadex LH-20 gel column in a mixture gradient of CH_3OH–H_2O (20%–100%) to give eight subfractions (Fr. V1–V8) [16]. Fr. V3 (9 g) was chromatographed on a small Sephadex LH-20 gel column using CH_3OH–H_2O (10%–30%) as eluent to yield 34 fractions (Fr. V3.1–V3.34). Fr. V3.13–Fr. V3.27 were combined and purified by semi-preparative HPLC with 45% CH_3OH–H_2O to yield **11** (58 mg) and **12** (94 mg). Fr. V4 (20 g) was chromatographed on a Sephadex LH-20 gel column using CH_3OH–H_2O (20%–30%) as eluent to yield 43 fractions (Fr. V4.1–V4.43). Fr. V4.20–Fr. V4.26 were combined and purified by semi-preparative HPLC with 40% CH_3OH–H_2O to yield **7** (20 mg). Fr. V5 (4.7 g) was further chromatographed on a small Sephadex LH-20 gel column using CH_3OH–H_2O (25%–40%) as eluent to generate 60 fractions (Fr. V5.1–V5.60). Fr. V5.44–Fr. V5.46 were combined and purified by semi-preparative HPLC with 20% CH_3CN–H_2O to yield **10** (13 mg). Fr. V7 (10.8 g) was chromatographed on a Sephadex LH-20 gel column using CH_3OH–H_2O (25%–40%) as eluent to yield 30 fractions (Fr. V7.1–V7.30). Fr. V7.16–Fr. V7.27 were combined and purified by semi-preparative HPLC with 40% CH_3OH–H_2O to yield **1** (96 mg), **2** (4 mg), **5** (14 mg) and **8** (15 mg). Fr. V8 (34.8 g) was chromatographed on a Sephadex LH-20 gel column using CH_3OH–H_2O (25%–50%) as eluent to yield 60 fractions (Fr. V8.1–V8.60). Fr. V8.27–Fr. V8.30 were combined and purified by semi-preparative HPLC with 45% CH_3OH–H_2O to yield **4** (6 mg). Fr. V8.31–Fr. V8.37 were combined and purified by semi-preparative HPLC with 45% CH_3OH–H_2O to yield **9** (590 mg). Fr. V8.38–Fr. V8.46 were combined and purified by semi-preparative HPLC with 45% CH_3OH–H_2O to yield **6** (7 mg) and **3** (12 mg).

2.5. Physicochemical and spectroscopic data of new compounds

2.5.1. Forsythenethoside C (1)

Brown amorphous powder; $[\alpha]_D^{20}$ −91.4 (*c* 0.10, CH_3OH); UV (CH_3OH) λ_{max} (log ε) nm: 218 (4.65), 293 (4.34), 331 (4.43) nm; IR (KBr) ν_{max} 3368, 2973, 1693, 1602, 1519, 1446, 1277, 1158, 1053 cm^{-1}; ^1H and ^{13}C NMR data (DMSO-d_6) see Table 1; HRESIMS *m/z* 1269.3833 $[M + Na]^+$ (calcd for $C_{58}H_{70}NaO_{30}$, 1269.3844).

2.5.2. Forsythenethoside d (2)

Yellow amorphous powder; $[\alpha]_D^{20}$ −65.0 (*c* 0.10, CH_3OH); UV (CH_3OH) λ_{max} (log ε) nm: 294 (4.23), 329 (4.37) nm; IR (KBr) ν_{max} 3342, 2970, 1695, 1598, 1516, 1452, 1232, 1157, 1046 cm^{-1}; ^1H and ^{13}C NMR data (DMSO-d_6) see Table 1; HRESIMS *m/z* 1151.3571 $[M + Na]^+$ (calcd for $C_{54}H_{64}NaO_{26}$, 1151.3578).

2.5.3. Forsythenethoside E (3)

Pale yellow amorphous powder; $[\alpha]_D^{20}$ + 7.4 (*c* 0.10 C_2H_5OH: H_2O 1:1); UV (CH_3OH) λ_{max} (log ε) nm: 330, 218; IR (KBr) ν_{max} 3346, 1697, 1603, 1518, 1446 cm^{-1}; CD (CH_3OH) λ_{max} nm ($\Delta\varepsilon$): 290 (+2.19), 238 (-9.67); ^1H and ^{13}C NMR data (DMSO-d_6) see Table 1; HRESIMS *m/z* 1269.3832 $[M + Na]^+$ (calcd for $C_{58}H_{70}NaO_{30}$, 1269.3844).

Table 1
The ^{1}H (500 MHz) and ^{13}C (125 MHz) NMR data of compounds **1**–**3** in DMSO-d_6.

	1		**2**		**3**	
No.	δ_H	δ_C	δ_H	δ_C	δ_H	δ_C
1		127.2		127.2		126.8
2	6.72, s	117.3	6.74, s	116.8	6.56, s	117.2
3		144.0		144.3		143.2
4		144.7		145.1		143.3
5	6.36, s	117.0	6.38, s	117.1	6.65, s	114.9
6		127.0		126.4		131.1
7a	2.55, m	32.5	2.51, m	32.7	2.73, m	32.2
7b	2.41, m					
8a	3.65, m	69.2	3.61, m	69.2	3.62, m	70.3
8b	3.44, m		3.43, m		3.53, m	
9		125.6		125.5		125.1
10	7.02, br s	114.8	7.01, br s	114.7	7.02, d (2.0)	114.6
11		145.6		145.7		145.6
12		148.5		148.8		148.9
13	6.74, d (8.0)	115.8	6.73, d (7.5)	115.8	6.73, d (8.0)	115.7
14	7.00, m	121.4	6.98, br d (7.5)	121.5	6.98, dd (8.0, 2.0)	121.4
15	7.47, d (16.0)	145.7	7.47, d (16.0)	145.8	7.48, d (16.0)	145.7
16	6.23, d (16.0)	113.8	6.23, d (16.0)	113.6	6.22, d (16.0)	113.4
17		165.8		165.8		165.8
18	4.16, d (8.0)	102.7	4.16, d (8.0)	102.7	4.23, d (8.0)	103.1
19	3.01, m	73.5	3.02, m	73.4	3.09, m	73.5
20	3.39, m	74.0	3.39, m	74.0	3.45, m	73.8
21	4.66, t (10.0)	71.7	4.66, t (9.5)	70.8	4.64, t (10.0)	71.0
22	3.53, m	72.8	3.46, m	72.7	3.56, m	73.0
23a	3.51, m	66.0	3.48, m	65.9	3.53, m	66.0
23b	3.28, m		3.24, m		3.34, m	
24	4.51, br s	100.6	4.43, br s	100.6	4.50, br s	100.3
25	3.57, m	70.3	3.54, m	70.3	3.59, m	70.1
26	3.40, m	70.6	3.37, m	70.6	3.40, m	70.6
27	3.14, m	71.9	3.11, m	71.9	3.13, m	71.9
28	3.41, m	68.4	3.35, m	68.4	3.37, m	68.4
29	1.02, d (6.0)	17.8	1.00, d (6.0)	17.7	1.02, d (6.0)	17.7
1′		129.2		128.9		133.5
2′	6.59, d (2.0)	116.3	7.01, br d (7.5)	129.8	6.54, d (2.0)	115.6
3′		145.0	6.60, dd (7.5, 2.5)	115.0		144.8
4′		143.5		155.5		143.5
5′	6.61, d (8.0)	115.5	6.60, dd (7.5, 2.5)	115.0	6.63, d (8.0)	115.3
6′	6.48, m	119.6	7.01, br d (7.5)	129.8	6.51, dd (8.0, 2.0)	119.0
7′a	2.67, m	35.1	2.71, m	34.8	4.19, m	44.7
7′b	2.67, m					
8′a	3.80, m	70.3	3.79, m	70.0	4.09, (m)	72.6
8′b	3.57, m		3.57, m		3.77, (m)	
9′		125.9		124.3		125.1
10′	6.48, d (1.5)	117.9	6.35, m	108.4	7.02, d (2.0)	114.6
11′		144.8		147.3		145.6
12′		147.5		137.5		148.9
13′	6.57, d (8.5)	115.3		147.3	6.73, d (8.0)	115.7
14′	6.43, dd (8.5, 1.5)	123.4	6.35, m	108.4	6.98, dd (8.0, 2.0)	121.4
15′	7.57, s	140.5	7.66, s	140.6	7.48, d (16.0)	145.7
16′		126.4		127.2	6.22, d (16.0)	113.4
17′		166.9		167.2		165.8
18′	4.28, d (8.0)	102.9	4.17, m	102.9	4.37, d (8.0)	103.0
19′	3.07, m	73.7	2.96, m	73.3	3.04, m	73.2
20′	3.34, m	74.2	3.40, m	76.5	3.42, m	73.9
21′	4.74, t (9.5)	70.9	3.14, m	70.1	4.67, t (10.0)	70.9
22′	3.48, m	72.6	3.34, m	73.8	3.62, m	72.8
23′a	3.51, m	65.9	4.54, br d (10.5)	64.1	3.55, m	66.0
23′b	3.29, m		4.05, m		3.32, m	
24′	4.42, br s	100.5			4.50, br s	100.4
25′	3.57, m	70.3			3.59, t (7.0)	70.2
26′	3.40, m	70.6			3.40, m	70.5
27′	3.14, m	71.9			3.15, m	71.8
28′	3.32, m	68.4			3.32, m	68.3
29′	1.08, d (6.0)	17.9			1.02, d (6.0)	17.7
11′–OCH_3			3.46, s	55.4		
13′–OCH_3			3.46, s	55.4		

2.5.4. Forsythoside Q (**4**)

Brown amorphous powder; $[\alpha]_D^{20}$ −47.0 (*c* 0.10, CH_3OH); UV (CH_3OH) λ_{max} (log ε) nm: 216 (4.55), 296 (4.41), 328 (4.56) nm; IR (KBr) ν_{max} 3355, 2969, 1703, 1630, 1600, 1516, 1448, 1272, 1159, 1043 cm^{-1}; ^{1}H and ^{13}C NMR (DMSO-d_6) see Table 2; HRESIMS *m/z* 785.2301 $[M-H]^-$ (calcd for $C_{38}H_{41}O_{18}$, 785.2298).

2.5.5. Forsythoside R (**5**)

Brown amorphous powder; $[\alpha]_D^{20}$ −81.1 (*c* 0.10, CH_3OH); UV (CH_3OH) λ_{max} (log ε) nm: 297 (4.25), 330 (4.37) nm; IR (KBr) ν_{max} 3396,

Table 2
The ^{1}H (500 MHz) and ^{13}C (125 MHz) NMR data of compounds **4**–**6** in DMSO-d_6.

	4		**5**		**6**	
No.	δ_H	δ_C	δ_H	δ_C	δ_H	δ_C
1		129.5		129.6		129.5
2	6.58, br s	115.7	6.57, d (2.0)	116.5	6.58, br s	115.8
3		144.9		144.8		144.9
4		143.4		143.4		143.5
5	6.57, m	116.4	6.58, d (9.0)	114.6	6.59, d (8.0)	115.8
6	6.38, m	119.4	6.34, m	119.5	6.37, br d (8.0)	119.5
7	2.48, m	34.8	2.51, m	34.7	2.50, m	34.7
8a	3.77, m	69.7	3.74, m	69.7	3.75, m	69.8
8b	3.36, m		3.48, m		3.46, m	
1′		125.5		125.6		125.3
2′	7.22, br s	110.9	7.22, d (2.0)	111.0	7.01, br s	114.3
3′		147.9		147.9		145.7
4′		149.4		148.6		148.8
5′	6.76, d (8.0)	115.3	6.76, d (8.5)	115.7	6.73, d (7.5)	117.2
6′	6.96, br d (8.0)	122.9	6.96, dd (8.5, 2.0)	123.0	6.96, br d (7.5)	121.6
7′	7.47, d (15.5)	144.9	7.47, d (15.5)	144.8	7.44, d (15.5)	144.9
8′	6.37, d (15.5)	114.9	6.38, d (15.5)	115.2	6.18, d (15.5)	113.1
9′		165.5		165.8		165.8
1″	4.17, d (7.5)	102.4	4.24, d (7.5)	101.8	4.23, d (8.0)	101.8
2″	2.99, t (7.5)	73.0	3.56, m	72.9	3.57, m	72.9
3″	3.36, m	73.7	3.66, m	78.9	3.67, m	78.8
4″	4.50, t (9.5)	71.1	4.56, t (10.0)	69.1	4.56, m	69.1
5″	3.49, m	73.4	3.12, m	74.3	3.14, m	74.4
6″a	3.58, br d (10.5)	68.0	3.56, m	68.0	3.55, m	67.9
6″b	3.37, m		3.35, m		3.36, m	
7″	4.42, d (8.0)	101.2	4.41, d (8.0)	101.2	4.42, d (7.5)	101.3
8″	4.61, t (8.0)	73.2	4.61, t (8.0)	73.2	4.60, m	73.2
9″	3.31, m	74.3	3.30, m	74.3	3.25, m	74.3
10″	3.32, m	69.7	3.32, m	69.7	3.31, m	69.7
11″a	3.73, m	65.7	3.72, m	65.6	3.71, m	65.7
11″b	3.08, m		3.08, m		3.08, m	
12″			4.96, br s	101.3	4.96, br s	101.2
13″			3.63, m	70.3	3.62, m	70.3
14″			3.31, m	70.4	3.26, m	70.4
15″			3.07, m	71.6	3.07, m	71.6
16″			3.29, m	68.8	3.31, m	68.8
17″			0.93, d (6.0)	18.2	0.91, d (6.0)	18.2
1‴		125.5		125.5		125.1
2‴	7.02, br s	114.6	7.01, d (1.5)	114.7	7.38, br d (8.5)	130.2
3‴		145.8		145.6	6.76, br d (8.5)	115.8
4‴		149.4		149.2		159.8
5‴	6.72, d (8.0)	115.5	6.73, d (8.0)	115.6	6.76, br d (8.5)	115.8
6‴	6.96, br d (8.0)	121.6	6.95, dd (8.0, 1.5)	121.6	7.38, br d (8.5)	130.2
7‴	7.44, d (16.0)	145.8	7.44, d (15.5)	146.0	7.46, d (16.0)	144.5
8‴	6.20, d (16.0)	113.3	6.18, d (15.5)	113.2	6.24, d (16.0)	114.3
9‴		166.0		165.5		165.5
3′–OCH_3	3.76, s	55.6	3.76, s	55.6		

2974, 1700, 1630, 1601, 1516, 1446, 1271, 1159, 1042 cm^{-1}; ^{1}H and ^{13}C NMR (DMSO-d_6) see Table 2; HRESIMS *m/z* 955.2847 $[M + Na]^+$ (calcd for $C_{44}H_{52}NaO_{22}$, 955.2842).

2.5.6. Forsythoside s (6)

Brown amorphous powder; $[\alpha]_D^{20}$ −19.4 (*c* 0.10, CH_3OH); UV (CH_3OH) λ_{max} (log ε) nm: 296 (4.16), 330 (4.23) nm; IR (KBr) ν_{max} 3367, 2973, 1707, 1630, 1603, 1516, 1446, 1264, 1164, 1044 cm^{-1}; ^{1}H and ^{13}C NMR (DMSO-d_6) see Table 2; HRESIMS *m/z* 925.2740 $[M + Na]^+$ (calcd for $C_{43}H_{50}NaO_{21}$, 925.2737).

2.6. Determination of the absolute configuration of sugars [17]

Compound **1** (4 mg) was dissolved in 0.1 M HCl (4 mL) and incubated under 70 ℃ for 6 h. The reaction mixture was concentrated to produce a residue. Then, the residue was suspended in H_2O and extracted with ethyl acetate for three times. The aqueous layer was evaporated under vacuum and dissolved in anhydrous pyridine (2 mL). L-Cysteine methyl ester hydrochloride (2 mg) was added, and the reaction was incubated for 1.5 h at 65 °C. Then, *N*-trimethylsilylimidazole (0.3 mL) was added in the mixture after the pyridine was dried. The reaction was maintained at 65 °C for 2 h and 2 mL H_2O was added in to quench the reaction. Finally, the reaction mixture was extracted by *n*-hexane (2 mL) for three times. Compounds **4** and **5** were treated as well as **1**. The *n*-hexane extracts were subjected to GC analysis under the conditions: capillary column, HP-5 (60 m × 0.25 mm, with a 0.25 μm film, Dikma); detection, FID; detector temperature, 300 °C; injection temperature, 300 °C; initial temperature, 200 °C, then raised to 260 °C at a rate of 10 °C/min; the final temperature was maintained for 30 min, then declined to 200 °C at a rate of 40 °C/min and the temperature was maintained for 1 min; carrier, N_2 gas. D-Glucose, L-rhamnose and D-xylose were confirmed by comparing the retention time of their derivatives with the original sugar treated in the same manner, which exhibited retention time of 29.5 min, 22.0 min and 19.0 min, respectively (Fig. S1, Supplementary material).

2.7. Neuroprotective assays of compounds 1–12

2.7.1. Rotenone induced PC12 cell damage [18]

Compounds **1**–**12** were tested for their neuroprotective activities against rotenone induced PC12 cell damage with an MTT assay. The PC12 cells were cultured in DMEM with 5% horse serum and 5% FBS.

100 μL of cells with a density of 5 × 10^4 cells/well were seeded in 96-well plates and incubated for 24 h at 37 °C under a 5% CO_2 atmosphere. The cultured cells were divided into four groups including the control group, the model group (4 μM rotenone), the positive control group (4 μM rotenone and 50 ng/mL nerve growth factor, NGF), and the sample group (4 μM rotenone and 10 μM test compounds), and then cultured for 48 h. 10 μL of MTT (0.5 mg/mL) was added to each well and maintained for 4 h before removing the medium. The formazan crystals were dissolved in DMSO and the absorbance was measured on a microplate reader at 550 nm. The cell viability (%) of each example was evaluated.

2.7.2. Serum-deprivation induced PC12 cell damage [19]

Compounds **1**–**12** were tested for neuroprotective activities against serum-deprivation induced PC12 cell damage with an MTT assay. The PC12 cells were cultured in DMEM with 5% horse serum and 5% FBS. Then, 100 μL of cells with an initial density of 5 × 10^4 cells/well were seeded in each well of a poly-L-lysine-coated, 96-well culture plate and cultured for 24 h at 37 °C under a 5% CO_2 atmosphere. The cells were incubated with or without test compounds (10 μM) in the medium without serum for 48 h afterwards. Then, 10 μL of MTT (0.5 mg/mL) was added and maintained for 4 h. The formazan crystals were dissolved in DMSO and the absorbance was measured on a microplate reader at 550 nm after removing the medium. The cell viability (%) of each example was evaluated.

2.8. Anti-inflammatory activities of compounds 1–12 [20]

The RAW264.7 cells were cultured in DMEM with 10% FBS under 5% CO_2 atmosphere at 37 °C for 12–18 h in 96-well plates. 80 μL of 2% FBS were added in each well after removing the supernate and cultured for 4 h. Then, the RAW264.7 cells were divided into four groups containing the control group, the model group (1 μg/mL lipopolysaccharide, LPS), the positive control group (1 μg/mL LPS and dexamethasone), and the sample group (1 μg/mL LPS and 10 μM test compounds), and cultured for 24 h. The supernatants of all groups were detected for TNF-α using commercially available solid-phase ELISA assay kits. Then, cell counting kit-8 (CCK8) was added in each well (10 μL/well) and incubated for 2 h. Finally, the absorbance was measured at 450 nm on a microplate reader and the concentrations of TNF-α were calculated through a standard curve. Inhibition (%) = (C_{model}-C_{sample})/ C_{model}*100%.

2.9. Statistical analysis

The neuroprotective assays were carried out three times with data reported as the mean ± standard deviation (SD). The significance level of differences in means was detected using the SPSS software with a one-way ANOVA. Statistical significances were defined at $p < 0.05$.

The anti-inflammatory tests were firstly carried out to get the preliminary screening data and then the active compounds were tested again to get the secondary screening data. The IC_{50} values were obtained from five level concentrations using the SPSS software.

3. Results and discussion

3.1. Structure determination of new and known compounds

The *n*-butanol portion of *F. suspensa* was separated by repeated column chromatography using macroporous adsorption resin and Sephadex LH-20 gel as fillers and subsequently purified by semi-preparative HPLC. As a result, forsythenethosides C–E (**1**–**3**), forsythosides Q–S (**4**–**6**), and six known compounds, including forsythenside K [21], isoacteoside [22], (*S*)-2-ethoxy-2-(3,4-dihydroxyphenyl)-ethyl-*O*-α-L-rhamnopyranosyl-(1 → 6)-4-*O*-*trans*-caffeoyl-β-D-glucopyranoside [23], suspensaside B [24], forsythenside J [21] and eutigoside B [25] were obtained (Fig. 1).

Compound **1** was isolated as a brown amorphous powder. Its molecular formula of $C_{58}H_{70}O_{30}$ was identified by the HRESIMS data at *m/z* 1269.3833 $[M + Na]^+$. The IR spectrum showed hydroxyl (3368 cm^{-1}), carbonyl (1693 cm^{-1}) and phenyl (1602 and 1519 cm^{-1}) groups. The ^1H

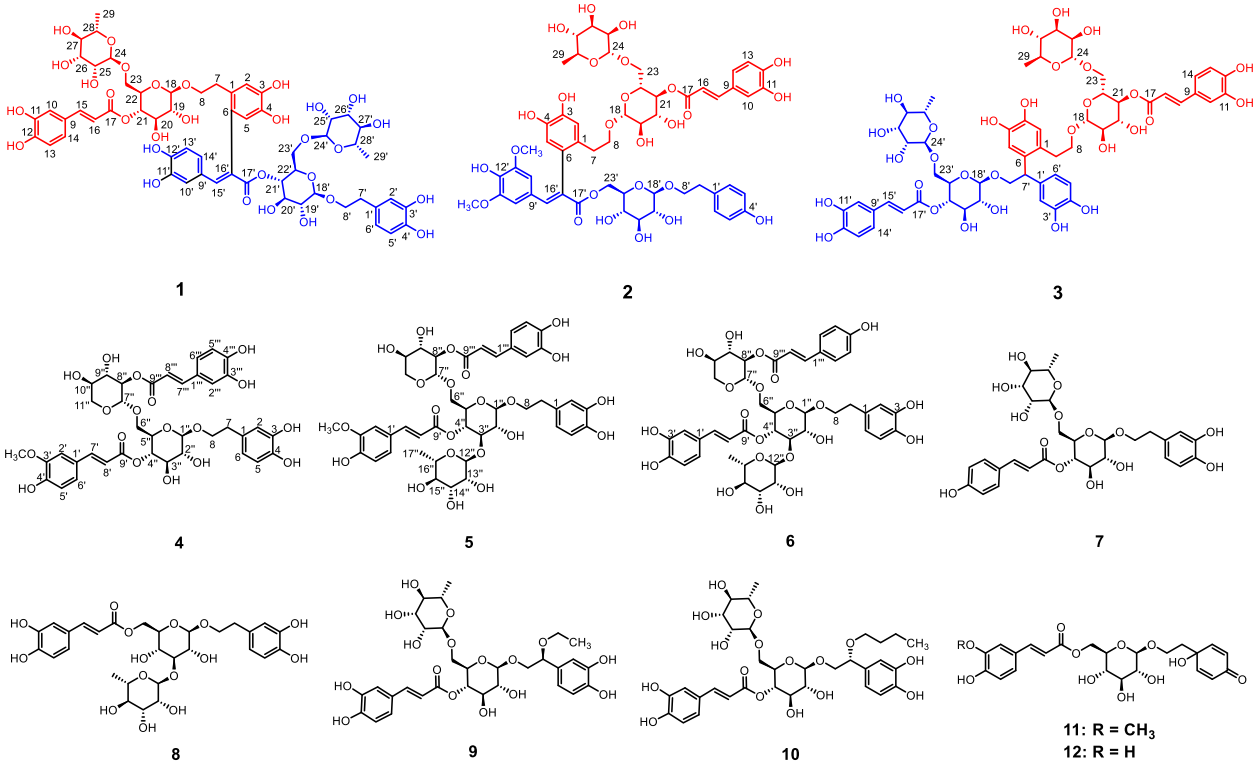

Fig. 1. Structures of compounds **1**–**12** isolated from the fruits of *F. suspensa*.

NMR data of **1** (Table 1) showed the presence of three sets of ABX systems at δ_H 7.02 (H-10), 6.74 (H-13), and 7.00 (H-14), 6.59 (H-2′), 6.61 (H-5′), and 6.48 (H-6′), and 6.48 (H-10′), 6.57 (H-13′) and 6.43 (H-14′), two *para*-aromatic protons at δ_H 6.72 (H-2) and 6.36 (H-5), and three olefinic protons at δ_H 7.47 (H-15), 6.23 (H-16), and 7.57 (H-15′). Two oxo-methylene signals at δ_H 3.65 (H-8a), 3.44 (H-8b), 3.80 (H-8′a), and 3.57 (H-8′b), and two methylene signals at δ_H 2.55 (H-7a), 2.41 (H-7b), and 2.67 (H-7′) were also observed. In addition, four aromatic protons at δ_H 4.16 (H-18, d, J = 8.0 Hz), 4.51 (H-24, br s), 4.28 (H-18′, d, J = 8.0 Hz) and 4.42 (H-24′, br s), along with 20 proton signals at δ_H 3.01–4.66 and two methyls at δ_H 1.02 (H-29) and 1.08 (H-29′) implied the presence of two β-glucoses and two α-rhamnoses. The ^{13}C NMR data of **1** showed 58 carbon signals, including 16 quaternary carbons, 34 methines, six methylenes, and two methyls. Among these signals, 24 carbons were attributed to the four sugars, and the remaining 34 carbon signals could be assigned to be two phenylethanoid moieties and two caffeoyl groups. Carefully analysis of the 1D NMR data of **1** suggested that it may be a homodimer consisted of two forsythoside A units, a main ingredient isolated from the fruits of *F. suspensa* [26]. It was confirmed by the HMBC correlations of H-18 with C-8, H-21 with C-17, H-24 with C-23, H-18′ with C-8′, H-21′ with C-17′ and H-24′ with C-23′ (Fig. 2). The C6–C16′ bond was located between the phenyl group and olefinic bond of the homodimer, which was confirmed by the HMBC correlations of H-5 with C-16′ and H-15′ with C-6 and the downshifting chemical shift values of C-6 (δ_C 127.0) and C-16′ (δ_C 126.4) compared to forsythoside A [26]. The $\Delta^{15'}$ olefin of compound **1** was assigned to be *E* geometry by the comparison of its NMR data at δ_H 7.57 (H-15′) and δ_C 140.5 (C-15′), 126.5 (C-16′) with that of previously reported forsythenethoside A at δ_H 7.68 (H-22) and δ_C 139.4 (C-22), 125.8 (C-23) [16]. Acid hydrolysis of **1** afforded two kinds of monosaccharides, and they were determined to be D-glucose and L-rhamnose by GC analysis compared to the authentic samples after derivation. Thus, the structure of compound **1** was determined as in Fig. 1 and named forsythenethoside C.

Compound **2** was isolated as a yellow amorphous powder. Its molecular formula was determined as $C_{54}H_{64}O_{26}$ by the positive HRESIMS ion peak at *m/z* 1151.3571 $[M + Na]^+$. Compared the 1D NMR data of **2** (Table 1) to that of **1** exhibited that they were very similar except for a few differences. The ^{1}H NMR data of **2** showed a set of AA′BB′ system at δ_H 7.01 (H-2′, H-6′) and 6.60 (H-3′, H-5′), and two *meta*-aromatic protons at δ_H 6.35 (H-10′ and H-14′), which replaced two sets of ABX systems in compound **1**. In addition, the presence of two methoxyl signals at δ_H 3.46 (11′–OCH_3, 13′–OCH_3) and the absence of a rhamnose moiety were observed. The ^{13}C NMR data of **2** showed 54 carbon signals, four carbons less than that of **1**, which was agreement with its ^{1}H NMR data. The HMBC correlations of H-18 with C-8, H-21 with C-17 and H-24 with C-23, and H-18′ with C-8′ and H-23′ with C-17′ confirmed the presence of a forsythoside A unit and another phenylethanoid glycoside moiety (Fig. 2). Its C6–C16′ bond was connected between the phenyl group and olefinic bond of the heterodimer, which was determined by the HMBC correlations of H-5 with C-16′ and H-15′ with C-6. Moreover, the connections of the two methoxyls were located at C-11′ and C-13′ confirmed by the correlations of 11′–OCH_3 with C-11′ and 13′–OCH_3 with C-13′. Thus, the structure of compound **2** was determined as shown in Fig. 1 and named forsythenethoside D.

Compound **3** was isolated as a pale yellow amorphous powder, and a molecula formula of $C_{58}H_{70}O_{30}$ was determined by its HRESIMS data at *m/z* 1269.3832 $[M + Na]^+$. Analysis of its ^{1}H and ^{13}C NMR data (Table 1) suggested that it was consisted of two forsythoside A units, the same with that of compound **1**. This was also been confirmed by the HMBC correlations of H-18 with C-8, H-21 with C-17, H-24 with C-23, H-18′ with C-8′, H-21′ with C-17′ and H-24′ with C-23′ (Fig. 2). The connection type of the two moieties was assigned between C-6 and C-7′ supported by the HMBC correlations of H-7′ with C-6 and H-7′ with C-1. It was confirmed by the downshfting chemical values of C-6 (δ_C 131.1) and C-7′ (δ_C 44.7) compared to forsythoside A [26]. The absolute configuration of C-7′ of **3** could not be assigned by comparison of the experimental and calculated ECD curves for the interference induced by the sugars and acyls. We tried to use acid and alkali hydrolysis to yield its aglycone, however, the aglycone was not obtained for complicated hydolysis products. Therefore, the absolute configuration of C-7′ was not determined. The structure of compound **3** was determined as shown in Fig. 1 and named forsythenethoside E.

Compound **4** was obtained as a brown amorphous powder. The HRESIMS negative ion peak at *m/z* 785.2301 $[M-H]^-$ suggested that its molecula formular was $C_{38}H_{42}O_{18}$. The IR sepctrum exhibted the presence of hydroxyl (3355 cm^{-1}), carbonyl (1703 cm^{-1}), and phenyl (1600 and 1516 cm^{-1}) groups. The ^{1}H NMR data of **4** (Table 2) displayed three sets of ABX systems at δ_H 6.58 (H-2), 6.57 (H-5), and 6.38 (H-6), 7.22 (H-2′), 6.76 (H-5′), and 6.96 (H-6′), and 7.02 (H-2‴), 6.72 (H-5‴) and 6.96 (H-6‴), two pairs of olefinic bonds at δ_H 7.47 (H-7′), 6.37 (H-8′), 7.44 (H-7‴) and 6.20 (H-8‴), two methylene groups at δ_H 2.48 (H-7), 3.77 (H-8a) and 3.36 (H-8b), and a methoxy group at δ_H 3.76 (3″–OCH_3). In

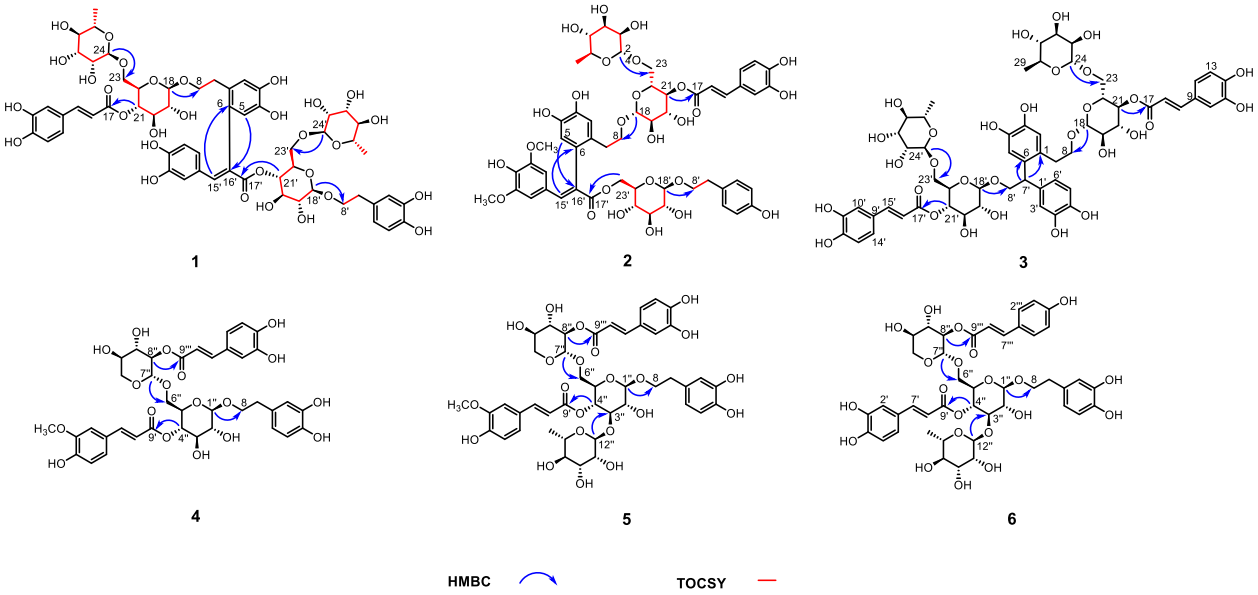

Fig. 2. The HMBC correlations (blue) of compounds **1**–**6** and the TOCSY correlations (red) of compounds **1**–**2**. (For interpretation of the references to colour in this figure legend, the reader is referred to the web version of this article.)

addition, two anomeric protons at δ_H 4.17 (H-1″, d, $J = 7.5$ Hz) and 4.42 (H-7″, d, $J = 8.0$ Hz), along with 11 protons between δ_H 2.99–4.61 suggested the presence of a β-glucose and a β-xylose. Its ^{13}C NMR spectrum showed 38 carbon signals, consisting of eight phenylethanoid carbon signals, nine caffeoyl carbon signals, 10 feruloyl carbon signals and 11 sugar carbon signals. The HMBC correlation of H-1″ with C-8 suggested the glucose linked on C-8 of the phenylethanoid moiety (Fig. 2). The xylose was attached on C-6″ of the glucose by the correlation of H-7″ with C-6″. The HMBC correlations of H-4″ with C-9′ and H-8″ with C-9‴ implied the feruloyl and caffeoyl groups were connected on C-4″ of the glucose and C-8″ of the xylose, respectively. Acid hydrolysis afforded two monosaccharides, which were determined to be D-glucose and D-xylose by GC analysis after derivation. Therefore, the structure of compound **4** was elucidated as shown in Fig. 1 and named forsythoside Q.

Compound **5** was isolated as a brown amorphous powder. Its molecula formula of $C_{44}H_{52}O_{22}$ was determined by the HRESIMS data at *m/z* 955.2847 $[M + Na]^+$. The structure of **5** was similar with that of **4** according to their 1D NMR data. The only difference between them was that an extra rhamnose was observed in **5**. The anomeric proton at δ_H 4.96 (H-12‴, br s), and the methyl signal at δ_H 0.93 (H-17‴) in ^{1}H NMR spectrum, along with six carbons at δ_C 101.3 (C-12‴), 70.3 (C-13‴), 70.4 (C-14‴), 71.6 (C-15‴), 68.8 (C-16‴), and 18.2 (C-17‴) in ^{13}C NMR spectrum supported the speculation (Table 2). The HMBC correlations of H-1‴ with C-8, H-4‴ with C-9′, H-7‴ with C-6‴ and H-8‴ with C-9‴ implied the connection type of **5** was the same with that of **4** (Fig. 2). Moreover, the cross-peak of H-12‴ with C-3‴ suggested the rhamnose was attached on C-3‴ of the glucose. Acid hydrolysis afforded three monosaccharides, which were determined to be D-glucose, D-xylose and L-rhamnose by GC analysis after derivation. Accordingly, the structure of compound **5** was elucidated as shown in Fig. 1 and named forsythoside R.

Compound **6** was isolated as a brown amorphous powder. The positive *quasi*-molecular ion peak at *m/z* 925.2740 $[M + Na]^+$ of the HRESIMS data suggested its molecular formula was $C_{43}H_{50}O_{21}$. Analysis of the 1D NMR data of **6** suggested it was much like that of **5** besides two small differences. The ^{1}H NMR data of **6** exhibited a group of AA′BB′ system signal at δ_H 7.38 (H-2‴, H-6‴) and 6.76 (H-3‴, H-5‴) and the absence of the methoxyl signal (Table 2). Combining with the HMBC cross-peaks of H-2′ with C-7′ and H-2‴ with C-7‴ suggested that the acyl groups in **5** were replaced by a caffeoyl group and a 4-hydroxylcinnamoyl group in **6** (Fig. 2). The connection type of **6** was the same with

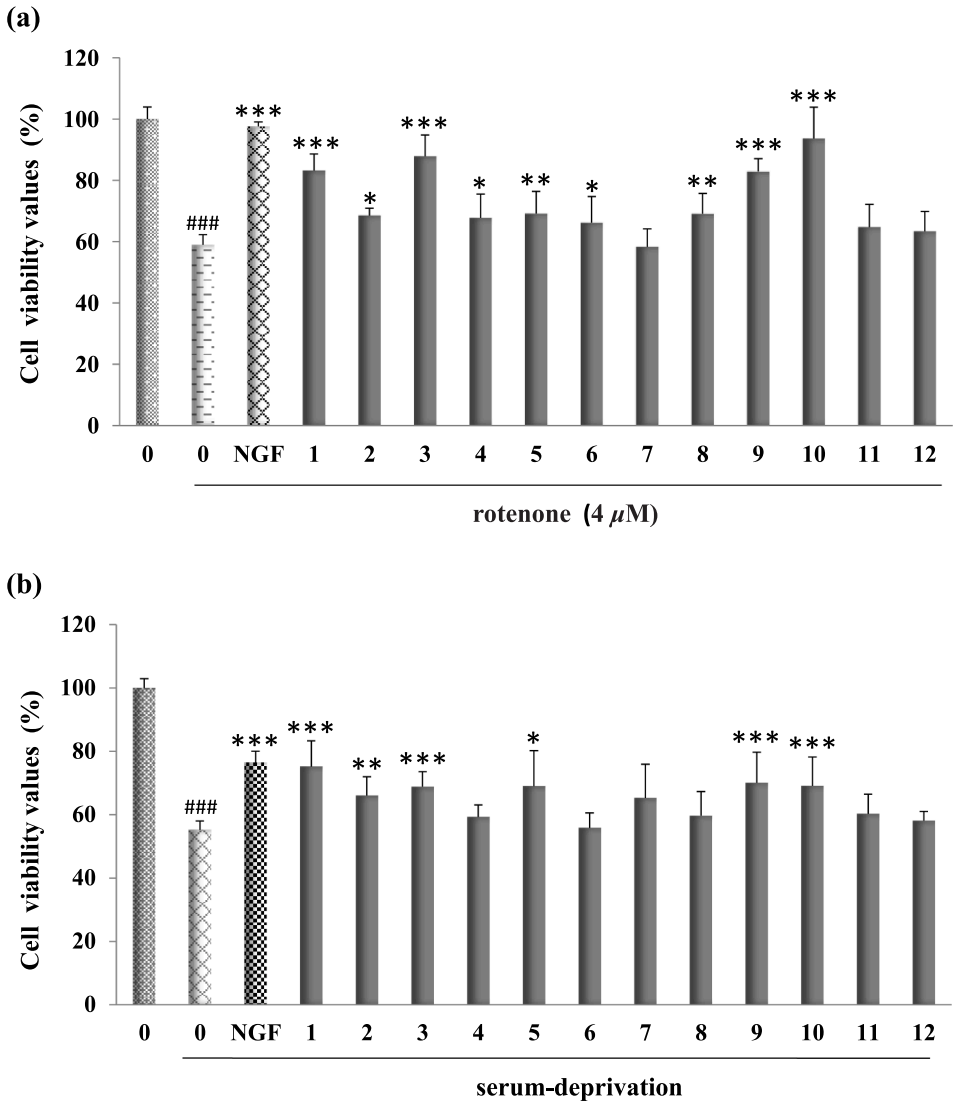

Fig. 3. (a) Neuroprotective activities of compounds **1**–**12** (10 μM) against rotenone induced PC12 cell damage. (b) Neuroprotective activities of compounds **1**–**12** (10 μM) against serum-deprivation induced PC12 cell damage. NGF: nerve growth factor, 50 ng/mL. The results are expressed as the means ± SD (n = 3). $^{###}p < 0.001$ (*vs.* control group), $^{*}p < 0.05$, $^{**}p < 0.01$, $^{***}p < 0.001$ (*vs.* model group).

that of **5** according to the correlations of H-1″ with C-8, H-4″ with C-9′, H-7″ with C-6″, H-12″ with C-3″ and H-8″ with C-9‴. Therefore, the structure of compound **6** was elucidated as shown in Fig. 1 and named forsythoside S.

3.2. Neuroprotective activities

All isolates (**1**–**12**) were evaluated for their neuroprotective activities against rotenone and serum-deprivation induced PC12 cell damage using nerve growth factor (NGF) as the positive control. As shown in Fig. 3**a**, compounds **1**–**6** and **8**–**10** showed obvious neuroprotective activities on the rotenone model at 10 μM. Notably, the cell viability value of **10** was reached to 93.65 ± 10.17%, which was very close to the positive control (NGF) with the cell viability value of 97.55 ± 1.48%. Additionally, compounds **1**, **3** and **9** showed strong activities with cell viability values over 80%. For the serum-deprivation model (Fig. 3**b**), the neuroprotective activities of test compounds were weaker than those of the rotenone model. Nevertheless, compound **1** exhibited almost the same cell viability value of 75.24 ± 8.05% at 10 μM, compared to that of NGF (76.47 ± 3.57%).

Carefully analysis of the structure–activity relationship of these isolates suggested that the phenylethanoid moiety and the caffeoyl group are essential for their neuroprotective activities. Meanwhile, the phenylethanoid moiety always connects on C-1 of the glucose and the caffeoyl group locates at C-4 or C-6 of the glucose. Sometimes, the caffeoyl group may appear at C-2 of the xylose, however, the rhamnose should have no substituents. In addition, diverse kinds, number or connection types of sugars and other acyl groups could also affect their bioactivities.

3.3. Anti-inflammatory activities

Compounds **1**–**12** were assayed on the inhibition of TNF-α expression induced by lipopolysaccharide (LPS) in mouse RAW 264.7 cells to assess their anti-inflammatory activities (**Tables S1 and S2, Supplementary material**). The result showed that compound **1** possessed excellent inhibition of TNF-α production with 89.28% at 10 μM, while, the positive control dexamethasone, with the inhibition of 82.50%. Compound **2** exhibited a moderate inhibition of 36.92%, however, the remaining 10 compounds only showed weak bioactivities against the LPS induced TNF-α expression. Further pharmacological research of compound **1** gave a remarkable IC_{50} value of 1.30 μM (dexamethasone, IC_{50}: 2.09 μM).

Based on the aforementioned bioactive data, phenylethanoid glycoside dimers possessed C6–C16′ bond seem more effective on inhibition of TNF-α production than C6–C7′ connected dimer as well as other phenylethanoid glycosides. Comparison of the structures of two C6–C16′ connected dimers indicates that the number of rhamnoses and the position of acyl groups may be important for their inhibitory effects.

4. Conclusion

In summary, this research was aimed to isolate and identify novel and bioactive phenylethanoid glycosides against neuroinflammation from the fruits of *F. suspensa*. As a result, 12 compounds including three unprecedented C6–C16′/C6–C7′ phenylethanoid glycoside dimers were obtained. Compounds **1** and **10** exhibited remarkable neuroprotective activities on serum-deprivation and rotenone induced PC12 cell damage, respectively. Moreover, compound **1** presented excellent inhibition of LPS induced TNF-α production in RAW 264.7 cells. The intriguing results suggested that the bioactive phenylethanoid glycosides might attenuate neuroinflammation and could bring us a unique perspective about the anti-neuroinflammatory effects of natural products.

Declaration of Competing Interest

The authors declare that they have no known competing financial interests or personal relationships that could have appeared to influence the work reported in this paper.

Acknowledgments

This research was financially supported by the National Natural Science Foundation of China (81673313) and the Innovation Fund for Medical Sciences (2016-I2M-1-010).

Appendix A. Supplementary data

Supplementary data to this article can be found online at https://doi.org/10.1016/j.bioorg.2021.105025.

References

[1] M.T. Heneka, M.P. Kummer, E. Latz, Innate immune activation in neurodegenerative disease, Nat. Rev. Immunol. 14 (2014) 463–477.
[2] S. Najjar, D.M. Pearlman, K. Alper, A. Najjar, O. Devinsky, Neuroinflammation and psychiatric illness, J. Neuroinflamm. 10 (2013) 43.
[3] G. Söderbom, B.Y. Zeng, The NLRP3 inflammasome as a bridge between neuroinflammation in metabolic and neurodegenerative diseases, Int. Rev. Neurobiol. 154 (2020) 345–391.
[4] S. Vetel, L. Foucault-Fruchard, C. Tronel, F. Buron, J. Vergote, S. Bodard, S. Router, S. Sérrière, S. Chalon, Neuroprotectve and ant-inflammatory effects of a therapy combining agonists of nicotnic α7 and σ1 receptors in a rat model of Parkinson's disease, Neural Regen. Res. 16 (2021) 1099–1104.
[5] L.K. Huang, S.P. Chao, C.J. Hu, Clinical trials of new drugs for Alzheimer disease, J. Biomed. Sci. 27 (2020) 18.
[6] H.J. Zhang, L. Bai, J. He, L. Zhong, X.M. Duan, L. Ouyang, Y.X. Zhu, T. Wang, Y. W. Zhang, J.Y. Shi, Recent advances in discovery and development of natural products as source for anti-Parkinson's disease lead compounds, Eur. J. Med. Chem. 141 (2017) 257–272.
[7] S.S. Zhang, Z.P. Yu, J.Y. Xia, X.M. Zhang, K.C. Liu, A. Sikd, M. Jin, Anti-Parkinson's disease activity of phenolic acids from *Eucommia ulmoides* Oliver leaf extracts and their autophagy activation mechanism, Food Funct. 11 (2020) 1425–1440.
[8] Q.Y. Tian, X.F. Fan, J.S. Ma, Y.J. Han, D.T. Li, S. Jiang, F.K. Zhang, H. Guang, X. Q. Shan, R. Chen, P. Wang, Q. Wang, J.G. Yang, Y.Y. Wang, L.G. Hua, Y.P. Shentu, Y.S. Gong, J.M. Fan, Resveratrol ameliorates lipopolysaccharide-induced anxiety-like behavior by attenuating YAP-mediated neuro-inflammation and promoting hippocampal autophagy in mice, Toxicol. Appl. Pharm. 408 (2020), 115261.
[9] X.L. Shang, Y.C. Shang, J.X. Fu, T. Zhang, Nicotine significantly improves chronic stress-induced impairments of cognition and synaptic plasticity in mice, Mol. Neurobiol. 54 (2017) 4644–4658.
[10] Chinese Academy of Sciences Flora of China Commission, Flora of China, Science Press, Beijing, 61 (2004) p. 42.
[11] Chinese Pharmacopoeia Commission, Pharmacopoeia of the People's Republic of China, China Medical Science Press, Beijing, 2015, p. 170 Part 1.
[12] S. Zhang, S.Y. Shao, X.Y. Song, C.Y. Xia, Y.N. Yang, P.C. Zhang, N.H. Chen, Protective effects of *Forsythia suspensa* extract with antioxidant and anti-inflammatory properties in a model of rotenone induced neurotoxicity, NeuroToxicology 52 (2016) 72–83.
[13] X.J. Yan, T.G. Chen, L.W. Zhang, H.Z. Du, Protective effects of forsythoside A on amyloid beta-induced apoptosis in PC12 cells by downregulating acetylcholinesterase, Eur. J. Pharmacol. 810 (2017) 141–148.
[14] F.G. Kong, X. Jiang, R.C. Wang, S.Y. Zhai, Y.Z. Zhang, D. Wang, Forsythoside B attenuates memory impairment and neuroinflammation via inhibition on NF-κB signaling in Alzheimer's disease, J. Neuroinflamm. 17 (2020) 305.
[15] F. Zhang, Y.N. Yang, X.Y. Song, S.Y. Shao, Z.M. Feng, J.S. Jiang, L. Li, N.H. Chen, P. C. Zhang, Forsythoneosides A-D, neuroprotective phenethanoid and flavone glycoside heterodimers from the fruits of *Forsythia suspens*a, J. Nat. Prod. 78 (2015) 2390–2397.
[16] S.Y. Shao, Z.M. Feng, Y.N. Yang, J.S. Jiang, P.C. Zhang, Forsythenethosides A and B: two new phenylethanoid glycosides with a 15-membered ring from *Forsythia suspensa*, Org. Biomol. Chem. 15 (2017) 7034–7039.
[17] S. Hara, H. Okabe, K. Mihashi, Gas-liquid chromatographic separation of aldose enantiomers as trimethylsilyl ethers of methyl 2-(polyhydroxyalkyl)-thiazolidine-4 *(*R)-carboxylatesi, Chem. Pharm. Bull. 35 (1987) 501–506.
[18] A.R. Im, Y.H. Kim, M.R. Uddin, S. Chae, H.W. Lee, Y.S. Kim, M.Y. Lee, Neuroprotective effects of *Lycium chinense* miller against rotenone-induced neurotoxicity in PC12 Cells, Am. J. Chin. Med. 41 (2013) 1343–1359.
[19] C.L. Zhang, Y. Wang, Y.F. Liu, G. Ni, D. Liang, H. Luo, X.Y. Song, W.Q. Zhang, R. Y. Chen, N.H. Chen, D.Q. Yu, Iridal-type triterpenoids with neuroprotective activities from *Iris tectorum*, J. Nat. Prod. 77 (2014) 411–415.
[20] Z.S. Wen, X.W. Xiang, H.X. Jin, X.Y. Guo, L.J. Liu, Y.N. Huang, X.K. OuYang, Y. L. Qu, Composition and anti-inflammatory effect of polysaccharides from *Sargassum horneri* in RAW264.7 macrophages, Int. J. Biol. Macromol. 88 (2016) 403–413.
[21] C. Li, Y. Dai, S.X. Zhang, Y.H. Duan, M.L. Liu, L.Y. Chen, X.S. Yao, Quinoid glycosides from *Forsythia suspensa*, Phytochemistry 104 (2014) 105–113.

[22] M.F. Shi, W.J. He, Y.L. Liu, X.R. Li, S.L. Yang, Q.M. Xu, Protective effect of total phenylethanoid glycosides from *Monochasma savatieri* Franch on myocardial ischemia injury, Phytomedicine 20 (2013) 1251–1255.
[23] S.Y. Shao, F. Zhang, Y.N. Yang, Z.M. Feng, J.S. Jiang, P.C. Zhang, An approach for determining the absolute configuration of C–2 in 2–oxygenated phenylethanoid glycosides by ^{1}H NMR spectroscopy, Org. Lett. 18 (2016) 4084–4087.
[24] D.S. Ming, D.Q. Yu, S.S. Yu, Two new caffeyol glycosides from *Forsythia suspensa*, J. Asian Nat. Prod. 1 (1999) 327–335.
[25] I.A. Khan, C.J. Erdelmeier, O. Sticher, New phenolic glucosides from the leaves of *Eurya tigang*, J. Nat. Prod. 55 (1992) 1270–1274.
[26] K. Endo, K. Takahashi, T. Abe, H. Hikino, Structure of forsythoside A, an antibacterial principle of *Forsythia suspensa* leaves, Heterocycles 16 (1981) 1311–1314.